

Application of Digital Speckle Correlation Method (DSCM) with 4 Nodes or 8 Nodes in the Wood Fracture Mechanics

Xiaomao Zhao^{1,2}, Ping Yang³, Dong Zhao^{1*}

¹School of Technology, Beijing Forestry University, Beijing

²College of Materials Science and Technology, Beijing Forestry University, Beijing

³Beijing Institute of Science and Technology Information, Beijing

CHINA

zhao_x_m@163.com, yangping_1989@163.com, zhaodong68@bjfu.edu.cn

*Correspondence: Dong Zhao

Abstract:-This article proposes a digital speckle correlation method (DSCM) displacement type based on finite element (FE) algorithm, in order to be suited for the irregular deformation and improve the precision of the DSCM. Both simulation and experiment processing, including three point bending deformation, show that the proposed method can achieve nearly the same accuracy as the finite element method in most cases and higher accuracy.

Key- Words: - Digital speckle correlation method, Finite element, Displacement type

1 Introduction

Two-dimensional digital speckle correlation method (2D-DSCM) is an effective optical measurement technique for full-field displacement and strain estimation, which has been widely used and recently become one of the most practical and flexible tools in the field of experimental mechanics and engineering measurement fields [1-3]. As compared to the special requirement of traditionally optical measurements, digital speckle correlation method is an easy and cheap method because it takes advantage of the speckle pattern on the specimen surface and only digital images taken by CCD camera are processed. The DSCM technique is predicated on the maximization of a correlation coefficient that is determined by examining the pixel intensity array subsets of two or more corresponding images and extracting the deformation type that relates the images to each other [4].

To establish correspondences between the undeformed and deformed speckle images, numerical techniques are used to locate an initially square image subset in a reference image within an image taken under load. During this process, displacement type of varying order can be applied to the initially square subset. Zero order displacement type permit the subset to translate rigidly, while first-order displacement type represent an affine transform of the subset that permits a combination of translation, rotation, shear and normal strains[5].

In this study, two new displacement types are introduced into DSCM in order to be suited for the irregular deformation and improve the precision of the DSCM according to the theories of the iso-parametric element in the finite element method.

2 Fundamental Theory

2.1 Principle of Digital Image Correlation

Through the gray variation of the undeformed and deformed speckle images in the surface of a specimen, the deformed information of specimen is got by DSCM. Its basic thoughts are that a rectangle subset is selected in the undeformed image and its gray information is used to look for the interactive place in the deformed image, lastly the displacement and strain of the searching point are got. A displacement type is essential to characterize the deformation of the deformed subset area, but for the complicated deformation, the general displacement types widely applied in DSCM cannot characterize the deformation of the subset area correctly, so the two new displacement types are introduced into DSCM in order to be suited for the irregular deformation and improve the precision of the DSCM according to the theories of the iso-parametric element in the finite element method (FEM).

2.2 Iso-parametric Element Displacement Type with 4 Nodes

Before presenting the quadrilateral elements, the appropriate natural coordinate system must be introduced for that geometry. The natural coordinates for a quadrilateral element are ξ and η , which are illustrated in Fig.1 for both straight sided or curved side quadrilaterals. These are called quadrilateral coordinates. These coordinates vary from -1 on one side to $+1$ at the other, taking the value zero over the quadrilateral medians.

In FEM derivations it is convenient to visualize

the quadrilateral coordinates plotted as Cartesian coordinates in the $\{\xi, \eta\}$ plane. This is called the reference plane. All quadrilateral elements in the reference plane become a square of side 2, called the reference element, which extends over $\xi \in [-1, 1], \eta \in [-1, 1]$.

According to the basic theories of the isoparametric element with 4 nodes in the finite element method (FEM), a local coordinate system $o\xi\eta$ is assigned to the centre of the square shown in Fig.1, which side length is 2. The angular points locations $(\xi_i, \eta_i) (i=1,2,3,4)$ are respectively $(\pm 1, \pm 1)$, so the equations of the square's sides are given in simple form of $\xi \pm 1 = 0$ and $\eta \pm 1 = 0$.

The displacement type is as follows:

$$\begin{cases} u = \sum_{i=1}^4 N_i u_i \\ v = \sum_{i=1}^4 N_i v_i \end{cases} \quad (i=1,2,3,4) \quad (1)$$

Where u_i, v_i are the displacement component of the node i .

The equation of shape functions as follows:

$$N_i = \frac{(1 + \xi_0)(1 + \eta_0)}{4} \quad (2)$$

Where $\xi_0 = \xi_i \xi, \eta_0 = \eta_i \eta$.

The transformation of coordinates is done by the regular square element as shown below:

$$\begin{cases} x = \sum_{i=1}^4 N_i x_i \\ y = \sum_{i=1}^4 N_i y_i \end{cases} \quad (i=1,2,3,4) \quad (3)$$

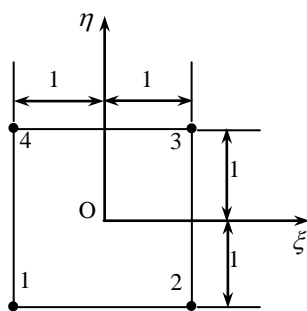


Fig.1 Mother element

The four angular points' coordinates (ξ_i, η_i) in the coordinate plane $\xi_o\eta$ in Fig.1 are mapped to the interactive angular points (x_i, y_i) in the coordinate plane xoy in Fig.2. Because the shape functions are bilinear, the mapped square in the coordinate plane $\xi_o\eta$ designs a quadrilateral element in which angular points are (x_i, y_i) . Distinctly, we can map all the points in the quadrilateral subsets to the square elements, which

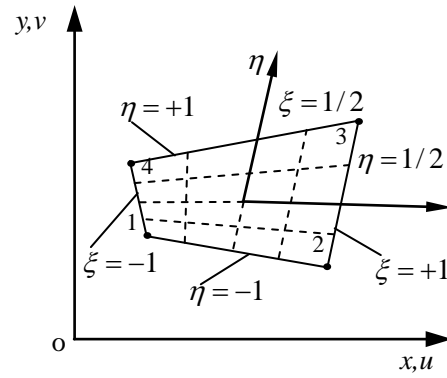


Fig.2 Quadrilateral elements

can be called mother element and looked on as a local coordinate system of the quadrilateral subset area. The local coordinate system defines the points in non-dimensional figure not to exceed 1, and its sides' equations are $\xi = \pm 1$ and $\eta = \pm 1$. From the theories of FEM, we can conclude that the upper displacement type is satisfied with the rule of maturity and compatibility.

From the equation 3, the transformation equation of the interactive points' location is obtained as follows:

$$\begin{cases} x^* = x + u^*(x, y) = x + \sum_{i=1}^4 N_i u_i \\ y^* = y + v^*(x, y) = y + \sum_{i=1}^4 N_i v_i \end{cases} \quad (4)$$

And equations mentioned above are introduced into the DSCM's formula, with which the correlated calculation is done. The displacement type is set in the local coordinate system, so that the coordinate transformation must be done during the calculation.

2.3 Iso-parametric Element Displacement Type with 8 Nodes

The mother element and the local coordinate system of the iso-parametric element displacement type with 8 nodes are shown in the Fig.3 and Fig.4. In comparison with the displacement type with 4 nodes, the displacement type with 8 nodes adds a middle node in each side.

The equation of shape functions is as follows:

$$N_i = \bar{N}_i - \sum_{i=1}^4 \bar{N}_i(\xi_{i+4}, \eta_{i+4}) N_{i+4} \quad (i=1,2,3,4) \quad (5)$$

Where,

$$\bar{N}_i = (1 + \xi_i \xi)(1 + \eta_i \eta) / 4 - (1 - \xi_i^2 \eta^2) / 2 \quad (i=1,2,3,4)$$

Where, $\xi_j, \eta_j (j=i+4=5,6,7,8)$ are local coordinates of nodes 5, 6, 7, 8.

$$N_1 = (1 + \xi_1 \xi)(1 + \eta_1 \eta) / 4 - (1 - \xi_1^2 \eta^2) / 2$$

$$\begin{aligned}
 N_2 &= (1 + \xi_2 \xi)(1 + \eta_2 \eta) / 4 - (1 - \xi^2 \eta^2) / 2 \\
 N_3 &= (1 + \xi_3 \xi)(1 + \eta_3 \eta) / 4 - (1 - \xi^2 \eta^2) / 2 \\
 N_4 &= (1 + \xi_4 \xi)(1 + \eta_4 \eta) / 4 - (1 - \xi^2 \eta^2) / 2 \\
 N_5 &= (\eta - 1)(\xi^2 - 1) / 2 \\
 N_6 &= (\xi + 1)(1 - \eta^2) / 2 \\
 N_7 &= (\eta + 1)(1 - \xi^2) / 2 \\
 N_8 &= (\xi - 1)(\eta^2 - 1) / 2
 \end{aligned}$$

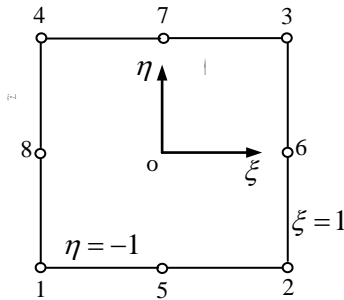


Fig. 3 Element with 8 nodes

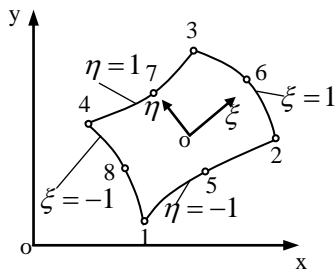


Fig. 4 Local coordinate elements

The format of linear combination is a merit, namely that it is convenient to generate the shape functions of the element s with 4,5,6,7 or 8 nodes. For example, the iso-parametric elements with nodes 5 and 7 are given in the formulas 4 and 5, only except that $N_5 = 0$.

From the shape functions, we can obtain the displacement type and coordinate transformation equations shown below:

$$\begin{cases} u = \sum_{i=1}^8 N_i u_i \\ v = \sum_{i=1}^8 N_i v_i \end{cases} \quad (6)$$

$$\begin{cases} x = \sum_{i=1}^8 N_i x_i \\ y = \sum_{i=1}^8 N_i y_i \end{cases} \quad (7)$$

From the equation 6, we can get the transformation equations of the two interactive points' locations:

$$\begin{cases} x^* = x + u^*(x, y) = x + \sum_{i=1}^8 N_i u_i \\ y^* = y + v^*(x, y) = y + \sum_{i=1}^8 N_i v_i \end{cases} \quad (8)$$

In addition, the displacement type is designed in the local coordinate system, so it must do coordinate transformation during the calculation. In comparison to the element with 4 nodes, the element with 8 nodes has 8 general coordinates. The displacement type with 8 nodes is added 4 nodes on the basis of the displacement type with 4 nodes. When the two ones are compared, we can conclude that the former is lower than the later, but its precision is slightly higher. In the paper the former is used to compute the deformed field near the crack tip of wood.

2.4 Two-dimensional Elastic Stress Analysis

Based on the von-Karman's geometrically non-linear theory, the strain-displacement relation can be expressed as

$$\varepsilon_{ij} = \frac{1}{2} \left[\frac{\partial u_i}{\partial x_j} + \frac{\partial u_j}{\partial x_i} \right]$$

It is assumed that the strain on the surface of specimen is plain strain and thus the three components of strain can be mathematically calculated from approximate curve as using following equations:

$$\begin{cases} \varepsilon_x = \frac{\partial u}{\partial x} \\ \varepsilon_y = \frac{\partial v}{\partial y} \end{cases}$$

The formulations for ε_x and ε_y are shown below in equation 9:

$$\begin{cases} \varepsilon_x = \frac{D_x(i-2, j) - 8D_x(i-1, j) + D_x(i+1, j) - D_x(i+2, j)}{12h_x} \\ \varepsilon_y = \frac{D_y(i-2, j) - 8D_y(i-1, j) + D_y(i+1, j) - D_y(i+2, j)}{12h_y} \end{cases} \quad (9)$$

where D_x and D_y are matrices of the x and y displacements, which are obtained by using DSCM, and h_x and h_y are the spacing of the control points in the x and y directions.

The stress-strain relation can be written as

$$\begin{cases} \sigma_x = \frac{E_x}{1 - \nu_{xy}^2} \varepsilon_x \\ \sigma_y = \frac{E_y}{1 - \nu_{yx}^2} \varepsilon_y \end{cases} \quad (10)$$

where E_x and E_y is the elastic modulus in the x and y directions, ν is the Poisson's ration. These elastic constants are obtained by using the principle

of electrical measure. The stress in two directions can be concluded from these calculations by using the displacement values from the DSCM analysis.

3 Results and Analysis

3.1 Wood Three-point Bending Fracture Experiment

In the section, a three-point bending fracture experiment of birch is done. Firstly, selecting a LT-veined birch specimen, the size of the specimen is shown in Fig.5, a mechanical crack was opened, 0.6mm in width, and then we went on to open a thinner crack with the help of the thin blade. Secondly the specimen was placed in the load frame shown in Fig. 6 and Fig.7, the undeformed and deformed speckle images were logged by CCD log system in Fig.8. Finally, the displacement field and strain field near the crack tip of birch were got by the DSCM of the 8 nodes-displacement type in the condition of temperature 10 °C and relative humidity 60%.

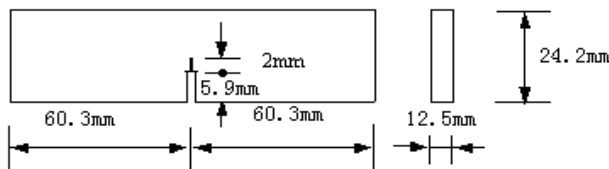


Fig. 5 Dimension of birch specimen with crack

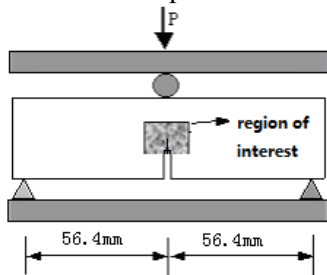


Fig.6 Load on view

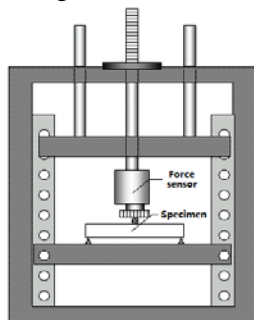
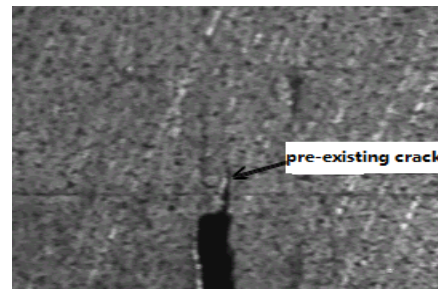
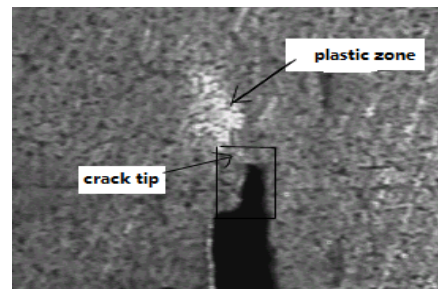


Fig.7 Device to load specimen



(a)



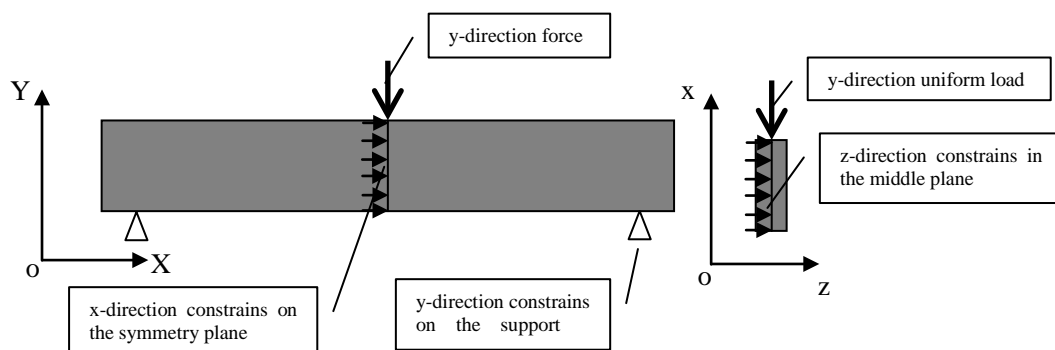
(b)

Fig.8 Original (a) and fractured (b) speckle images

After we got two good speckle images, the displacement and strain field were obtained by the DSCM. Because the data errors lied, the data must be done with for the second time. Firstly, we transformed the data field to the digital image, and then used the image smooth method to filter the noise for lots of times, lastly transformed the filtered image to the displacement and strain data field back.

3.2 Numeric Simulation of the Wood Three-bending Fracture Experiment

Additionally, in the paper the software ANSYS was used to compute and analyze the displacement and strain field near the crack tip of birch and the results got by software ANSYS were compared with the result got by DSCM. According to birch vein directions and load type, the birch specimen was simplified to the orthotropic material model. The L direction of the specimen was defined as X axis, the T direction as Y axis and the R direction as Z axis in the ANSYS model. The boundary conditions are shown in the Fig.9.



(a) Project of the *xoy* plane in *z* direction

(b) Project of the *xoz* plane in *y* direction

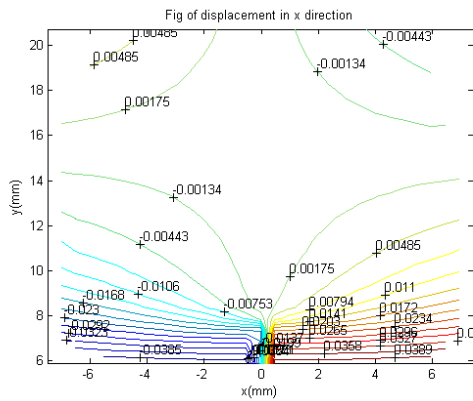
Fig.9 Boundary conditions in 3d model

4 Conclusion

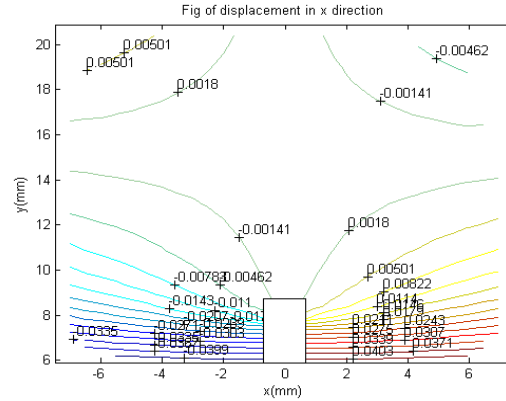
During the correlated calculation, the size of the subset area is 21×21 pixels. Because of the discontinuation at the crack tip, about 10 pixels area near the crack tip was not be computed and 15 pixels area near the crack tip was removed. In the below Figures, the blank area bracketed in the black line was the removed one. The experimental results

were done in different load conditions, but only the P=600N result was select to be shown in Fig.10.

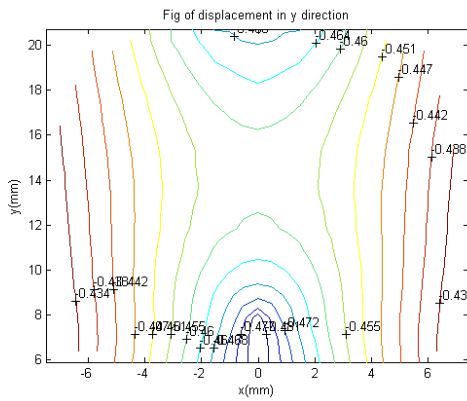
Fig.10 (b)、(d)、(f)、(h) shows the displacement fields and the normal stress by using the DSCM based on the equation 8-10, the FEM simulation results of which are shown in Fig.10 (a)、(c)、(e)、(g).



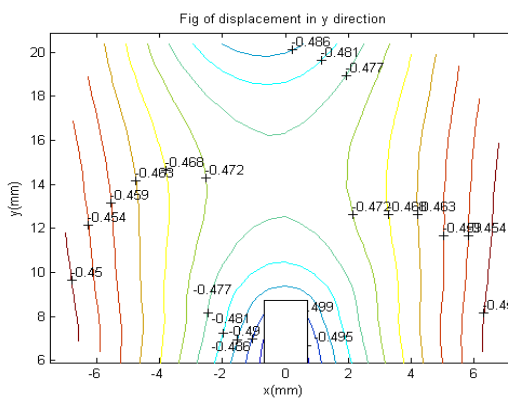
(a) *x*-directed displacement in FEM *u*(mm)



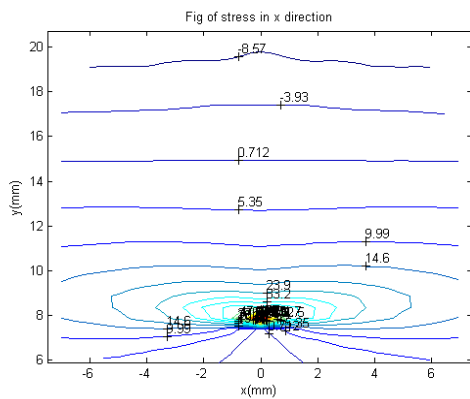
(b) *x*-directed displacement in DSCM *u*(mm)



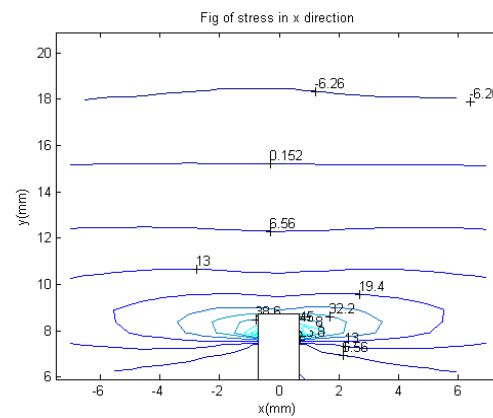
(c) *y*-directed displacement in FEM *v*(mm)



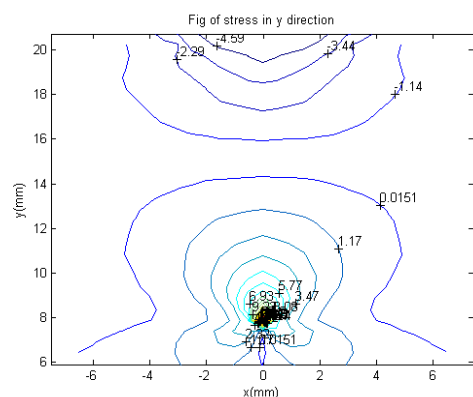
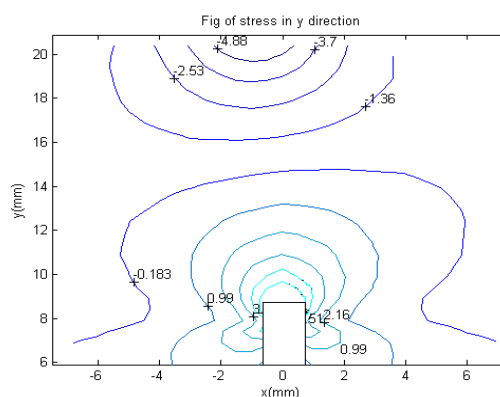
(d) *y*-directed displacement in DSCM *v*(mm)



(e) *x*-directed normal stress in FEM σ_x (MPa)



(f) *x*-directed normal stress in DSCM σ_x (MPa)

(g) y-directed normal stress in FEM σ_y (MPa)(h) y-directed normal stress in DSCM σ_y (MPa)Fig.10 Comparison of two methods results when $P=600N$

For the displacement field, the two methods results are basically same in the changed trend, and the one's value approaches the other; for the stress field, there are some difference, their changed trend are same, and the values is different, but there is the same numeric order. It is possible that the formula of the strain is the derivative of displacement, the strain polynomial expression is lower one order than the displacement type; for the shear stress, the result of the two methods are more different, but basically we can recognize the changed trend. In words, the two methods are basically coincident, and the two new displacement types given out in this paper are stable and reliable in DSCM.

Reference:

- [1] M. A. Sutton, J. J. Orteu, and H. W. Schreier, *Image Correlation for Shape, Motion and Deformation Measurements: Basic Concepts, Theory and Applications*, Springer, New York, USA, 2009.
- [2] B. Pan, K. Qian, H. Xie, and A. Asundi, Two-dimensional digital image correlation for in-plane displacement and strain measurement: a review. *Measurement Science and Technology*, Vol.20, No. 6, 2009.
- [3] M. Malesa, M. Kujawińska, Deformation measurements by digital image correlation with automatic merging of data distributed in time, *Applied Optics*, Vol.52, 2013, pp. 4681-4692.
- [4] Z. Jian, Z. Dong, and Z. Zhe, Assessment of

Gradient-Based Digital Speckle Correlation Measurement Errors, *Journal of the Optical Society of Korea*, Vol.16, 2012, pp. 372-380.

[5] Z. Jian, Z. Dong, and Z. Zhe, "A Non-Contact Varying Temperature Strain Measuring System Based on Digital Image Correlation" ,*Experimental Techniques*, Online, 2013.

[6] R.J. Sanford, Determining fracture parameters with full-field optical methods, *Experimental Mechanics*, Vol. 29,1989, pp. 241-247.

[7] Y.Q. Wang, M. A. Sutton, H.A. Bruch, and H. W. Schreier, Quantitative error assessment in pattern matching: effects of intensity pattern noise, interpolation, strain and image contrast on motion measurement, *Strain*, Vol. 45, 2009, pp. 160-178.

[8] B. Pan, H. M. Xie, Z. Y. Wang, K. M. Qian, and Z. Y. Wang, Study on subset size selection in digital image correlation for speckle patterns, *Optics Express*, Vol. 16, No.10, 2008, pp.7037-7048.

[9] H.W. Schreier, J.R. Braasch, M.A. Sutton, Systematic errors in digital image correlation caused by intensity interpolation, *Optical Engineering*, Vol. 39, No. 11, 2000, pp. 2915-2921.

[10] P.L. Reu, Experimental and Numerical Methods for Exact Subpixel Shifting, *Experimental Mechanics*, Vol.51, 2011, pp. 443-452.

[11] B. Pan, H. Xie, B. Xu, and F. Dai, Performance of sub-pixel registration algorithms in digital image correlation. *Measurement Science and Technology*, Vol. 17, 2006, pp. 1615-1621.